

# Design of a blue LED stimulation unit with a highly uniform illumination pattern

I. Quesada, M.R. Otazo, L. Baly\* and Y. Gonzalez

Centro de Aplicaciones Tecnológicas y Desarrollo Nuclear (CEADEN) AP 6122, Miramar, La Habana, Cuba.

(\*Corresponding author: baly@ceaden.edu.cu)

(Received 11 November 2004; in final form 8 December 2004)

## Abstract

The current study is concerned with the design and construction of a blue LED stimulation unit with a highly uniform illumination pattern. The pattern produced by a single LED is characterized experimentally. Using this information and making certain approximations, the illumination pattern produced by an array of LEDs was computer generated, and the mean intensity and relative standard deviation were calculated. In this way, several hypothetical configurations were evaluated; the most convenient configuration was constructed and experimentally characterized. The measured uniformity expressed as the relative (to the mean intensity) standard deviation in the sample zone was as good as 1.7%.

## Introduction

Quartz photoluminescence is being widely employed for dating and retrospective dosimetry. This has encouraged the development of reliable reading systems, with emphasis on improvements in the detection system, the stimulation unit, the electronics and the ionizing radiation source. The stimulation unit is an essential part of any photoluminescence reading system and it should supply radiation with an appropriate power density that is both spectrally and temporally stable. With such an aim halogen lamps, ultra-bright green and blue LEDs (Bøtter-Jensen, 2000; Bøtter-Jensen and Murray, 1999; Bøtter-Jensen et al., 1999) and more recently, solid state lasers (Duller et al., 2000) have been employed. Figure 1 shows the standard configuration used to measure the photoluminescence; a photomultiplier tube faces a sample of quartz crystals that are spread over a 1cm-diameter metallic disk.

Ultra-bright LEDs have several advantages over other classes of light sources. They have the features of a solid state device such as compactness, robustness, long life, low power consumption and low cost. Compared with ultra-bright green LEDs, blue LEDs are more efficient at producing

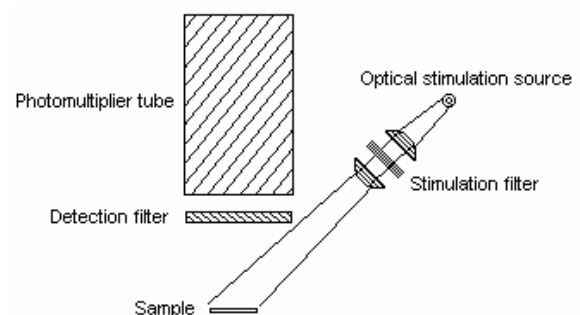


**Figure 1:** Standard configuration of a photoluminescence reading system

photoluminescence (Bøtter-Jensen, 2000) and thus they have been extensively studied for this application (Bøtter-Jensen and Murray, 1999; Bøtter-Jensen et al., 1999). These studies demonstrated the high spectral and temporal stabilities of these devices. The selection of the specific arrangement of the LEDs has been guided mainly by the requirement of producing a given power density at the sample.

Recent reports have drawn attention to the fact that only a small percentage of quartz crystals show effective photoluminescence (Duller et al., 2000; Jacobs et al., 2003). In the case of multi-crystal samples, these bright crystals are randomly distributed in the sample holder and their exact position will be different every time the position of the sample disc is changed on the holder. This may become a serious source of variability if the pattern of illumination at the sample is not uniform. Since the luminescence signal is determined by the intensity of the stimulation radiation received by each crystal, the luminescence signal will depend on the position of these bright crystals in relation to the illumination pattern.

In the present work, the design of a blue LED stimulation unit is described, and in addition to the general requirements, special significance is given to

the production of a highly uniform illumination pattern. To achieve this, the illumination pattern of a single LED was experimentally characterized, and these data were used to develop a computer code to generate the illumination pattern of an hypothetical array of LEDs. For each generated pattern, the mean intensity and standard deviation (uniformity) were calculated, and several configurations were evaluated. The most convenient configuration was constructed and experimentally characterized.

### Starting design considerations

The power density of typical configurations based on blue LEDs has been reported to be in the range of 20 - 40 mW/cm<sup>2</sup> (Bøtter-Jensen, 2000) and the current stimulation unit is planned to produce similar levels of power density. The illumination uniformity will be evaluated as the relative standard deviation of the radiation intensity across the sample. At the moment, there is no strong criterion that leads to the selection of uniformity; however, a 10% standard deviation will be taken as the guiding parameter.

First, the performance characteristics of a blue LED were analyzed. The maximal power emitted by an ultra-bright blue LED is about 2 mW; thus, a minimum number of 20 LEDs will be needed to match the highest power density reported in the literature. Second, the illumination pattern produced by a single LED is not uniform. Notable differences between the intensities at the spot center and the borders are observed (Figure 2). Therefore, even when several LEDs are arranged appropriately, producing a highly uniform pattern seems to be complicated.

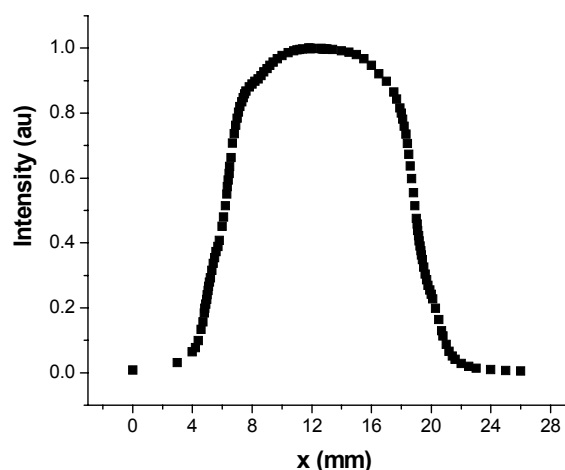


**Figure 2:** Illumination pattern produced by an ultra-bright blue LED.

### Proposed solution

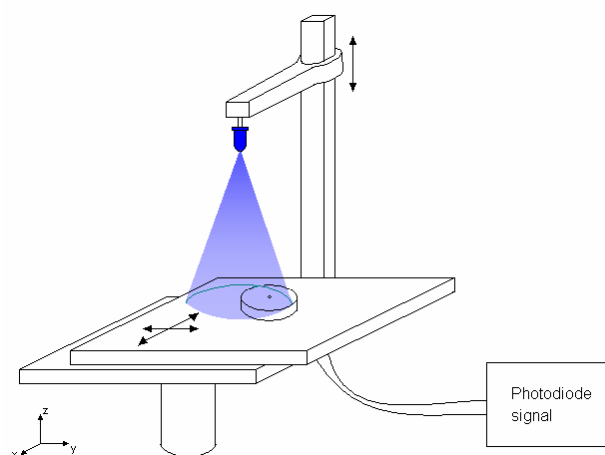
To resolve this problem, sample illumination using only part of the illuminated area will be used. The boundaries of such a region will be determined by a cut-off relative intensity; in our case, this region is defined by the points whose intensity is higher than  $0.9 I_{\max}$ , hereafter the 90% cut-off region.

To implement such an idea, two problems need to be solved. First the distance between the LED and the sample, for which the sample will be illuminated with the 90% cut-off region, should be determined. Unfortunately, the viewing angle reported by the LED manufacturer corresponds to the 50% cut-off region, and can not be used for our purposes. Therefore, a detailed study of the illumination pattern for different distances between the LED and the sample should be made.

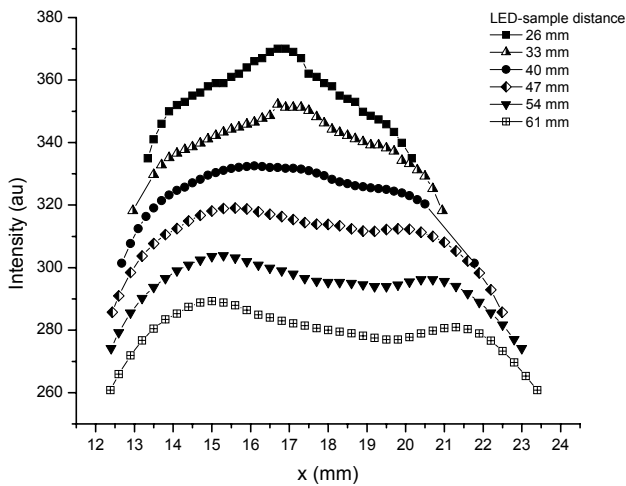
Second, under the new conditions the power delivered to the sample will be less than the total one, and therefore, the percentage of the total power contained within the 90% cut-off region needs to be found. This parameter will be important for determining the number of LEDs required to achieve the planned power density.

### Experimental

Figure 3 shows the experimental setup employed to characterize the illumination pattern. The LED was fixed to a variable length arm and a photodiode with a 0.3 mm-diameter collimator was mounted in a dual axis X-Y micropositioning system. An electronic module attached to the system allowed the reading of the photodiode position with a precision of 10  $\mu\text{m}$ .

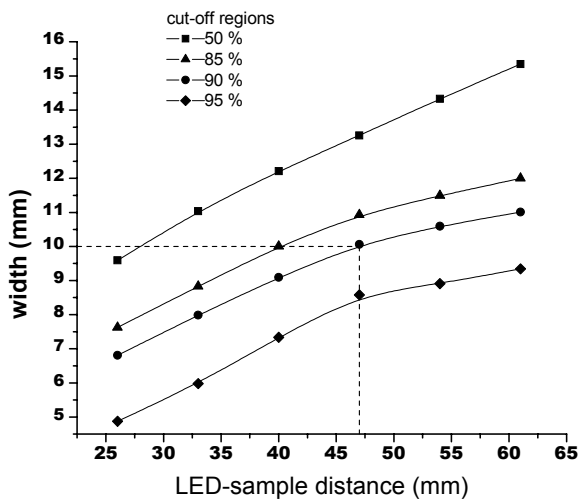


**Figure 3:** Experimental setup to measure the illumination pattern of a single LED.



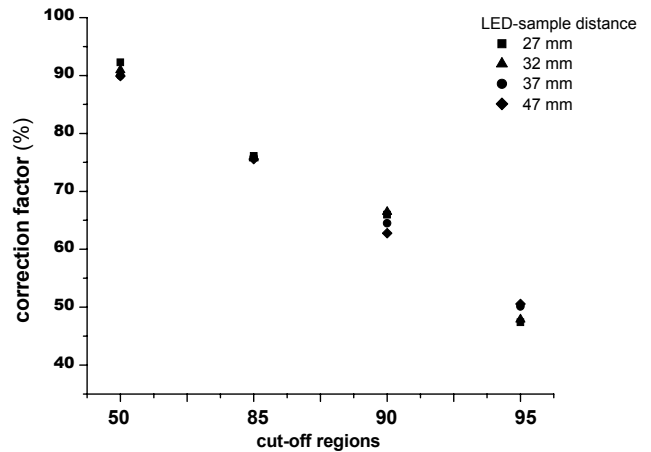
**Figure 4:** Measured distribution of intensity in a single axis for different distances between the LED and the photodiode.

Figure 4 shows the measured distribution of intensity in a single axis for different distances (from 26 mm to 61 mm) between the LED and the photodiode; note that only the 90% cut-off region is shown. From these data, a new graphic (Figure 5) was constructed to reflect the dependence of the geometrical width of several cut-off regions for different distances between the LED and the photodiode.



**Figure 5:** Geometrical width of several cut-off regions for different distances between the LED and the photodiode.

Finally, from the experimental data, the percentage of the power contained in each cut-off region for different distances was calculated (Figure 6). The percentage was determined as the ratio of the area included in the cut-off region to the whole distribution area.



**Figure 6:** Power correction factor in each cut-off region for different distances.

At this point some important conclusions can be presented:

1. For a normal angle of illumination and a distance of 47 mm between the LED and the 10 mm diameter sample, the latter is totally illuminated by the 90% cut-off region, as shown by the lines drawn in Figure 5. When the distance is less, the sample area is not illuminated with greater than 90% of maximal power.
2. Under these conditions, the power delivered to the sample will be approximately 60% of the total (Figure 6).
3. Considering a sample area of 0.78 cm<sup>2</sup> (i.e. with diameter of 10 mm) illuminated by the 90% cut-off region and a maximal output power for a blue LED of 2 mW, the planned power density of 40 mW/cm<sup>2</sup> in the sample zone will be reached with a minimum of 26 LEDs.

**Procedure for the pattern generation of the LED configuration**

The next step in the construction of the stimulation units is the selection of the LED configuration. The LED configuration is defined by the number of LEDs, their orientation and distribution, but the number of possible configurations is huge.

The application of an empirical method to select the best configuration has several drawbacks. First, the mechanical support for the LEDs is difficult to construct as a flexible test rig, and second, there is no procedure for the evaluation in advance of the sample illumination uniformity. Instead, we chose to compute the illumination pattern produced by an hypothetical array of LEDs and then selected the most suitable configurations using a program based on the MatLab 5.3 code.

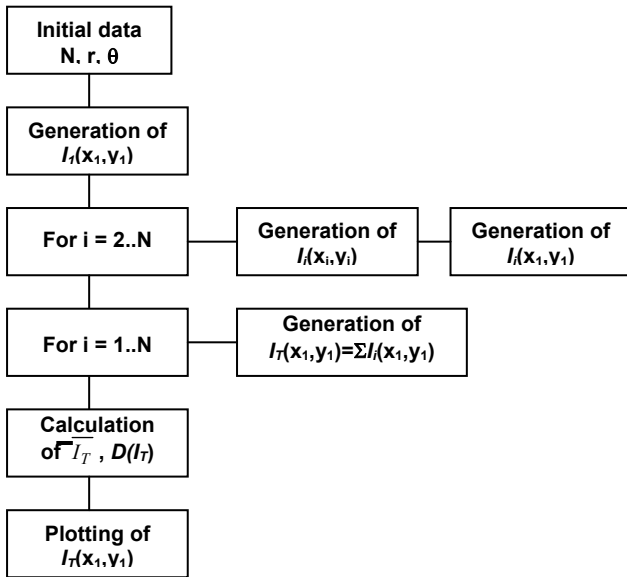


Figure 7: General algorithm used to generate the illumination pattern of an array of LEDs.

Figure 7 shows the general algorithm used to generate the illumination pattern of an array of LEDs. First, the pattern of the first LED  $I_1(x_1, y_1)$  is computer generated. Then, the pattern of the following LED  $I_i(x_i, y_i)$  ( $i = 2..N$ ) is generated and interpolated to the coordinate system of the first LED  $I_1(x_1, y_1)$ . This procedure is performed for each LED after which the array pattern  $I_T$  is calculated by summing all individual patterns  $I_i(x_1, y_1)$  ( $i = 1..N$ ). Finally, the mean intensity  $\bar{I}_T$ , and the standard deviation  $D(I_T)$  are calculated for later comparison.

**Single LED pattern generation module**

From this algorithm, it can be seen that the single LED pattern generation plays an important role. The heart of this module is a sub module whose function is to calculate the radiation intensity at any point within the space limited by the following conditions:  $-7 \text{ mm} < x < 7 \text{ mm}$ ,  $-7 \text{ mm} < y < 7 \text{ mm}$ ,  $47 \text{ mm} < z < 61 \text{ mm}$ , where  $z$  is the distance between the LED and the sample when the illumination is performed at a normal angle. To calculate the intensity, this sub module uses the intensity distribution measured with

a space resolution  $\Delta x = \Delta y = 0.3 \text{ mm}$  in three different planes A( $z=47$ ), B( $z=54$ ) and C( $z=61$ ) (Figure 8). Then assuming that for every pair  $x, y$  the intensity varies linearly as  $z$ , the intensity at any point  $I(x, y, z)$  is calculated as the linear interpolation of  $I(x, y, z_A)$ ,  $I(x, y, z_B)$  and  $I(x, y, z_C)$ .

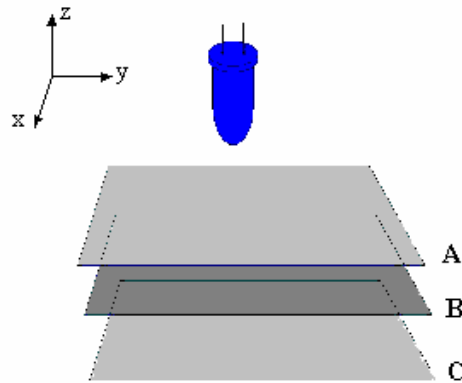


Figure 8: Schematic representation of the three geometrical planes where the intensity was measured.

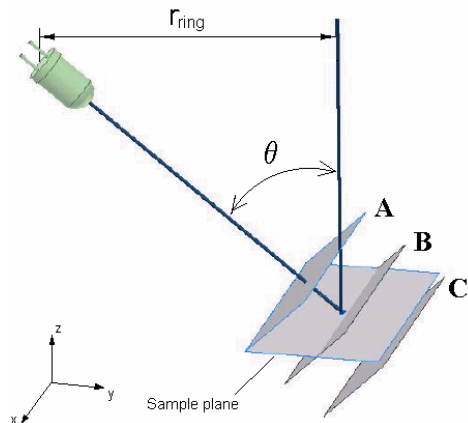


Figure 9: Schematic representation of the three geometrical planes where the intensity was measured in relation to the sample plane.

There is a second sub module which, depending on the LED position and orientation, determines the points of the sample plane in the LED coordinate system (Figure 9). For calculations it is considered that the LED is aligned parallel to the  $y$  axis and that the interception of such a line with the sample plane occurs at  $x = 0$ . The origin of the sample coordinate system is located on its center. The LED position and orientation is defined by two parameters: the angle  $\theta$  and the distance  $r$ ; the first is the angle between the

normal to the sample plane and the direction of the LED alignment, the second is the LED y-coordinate. After introducing the parameters  $\theta$  and  $r$ , this module checks that such a combination is geometrically consistent with the requirement that the distance between the sample and the LED is 47 mm. When successful, it generates the illumination pattern produced by such an LED in the sample plane.

**Selection of the LED configuration**

Figure 10 shows the model that was used for each evaluated configuration. The LEDs are distributed in two concentric rings of 20 LEDs each. The total number of LEDs (40) is higher than previously calculated; however, in this configuration the LEDs will not be subjected to extreme operating conditions. Each ring is characterized by its radius  $r$  and angle  $\theta$ .

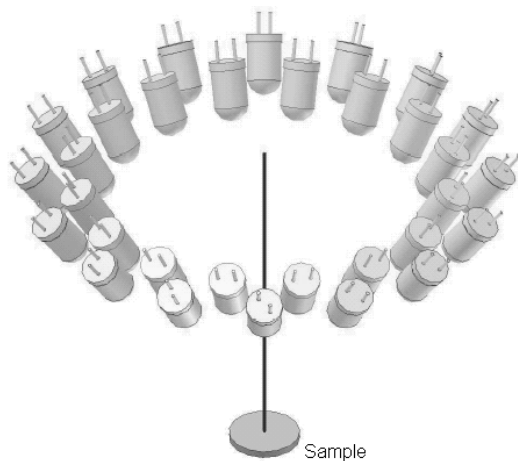


**Figure 10:** Model for the evaluated positions.

Using the design program AUTOCAD and considering the minimal distance between the LED and the sample as well as the dimensions of the photomultiplier tube, the range of possible values for the radius of the ring was determined. Starting from  $r = 22$  mm and incrementing the radius in steps of 0.5 mm, a set of radii was defined. For each predefined radius  $r$  and different values of  $\theta$ , the pattern produced by each ring was generated and visually evaluated. The mean intensity and the standard deviation were also calculated. For each radius, the angle  $\theta$  producing the pattern with the smallest standard deviation was selected. Once again, using the program AUTOCAD, proposed configurations were evaluated, but this time considering the real LED dimensions. From this analysis two configurations were selected (Table 1).

$r(\text{mm})$	$\theta$	$D(I_T)$	$\overline{I_T}$	$I_T \text{ max}$	$I_T(0,0)$
28.0	32.0	2095.1	95642	98711	98658
35.0	39.5	1484.7	95171	97073	97073

**Table 1:** Parameters of the two selected configurations.

**Construction and evaluation of the stimulation unit**

Using the results of the previous section, the stimulation unit was designed and constructed (Figure 11). Before the LEDs were mounted, the power output of each LED was determined (Figure 12) and they were found to vary by up to 30%. To minimize any effects, LEDs with similar outputs were mounted in the inner ring; the rest were mounted in the outer ring, alternating one LED of low output with another one of high output.

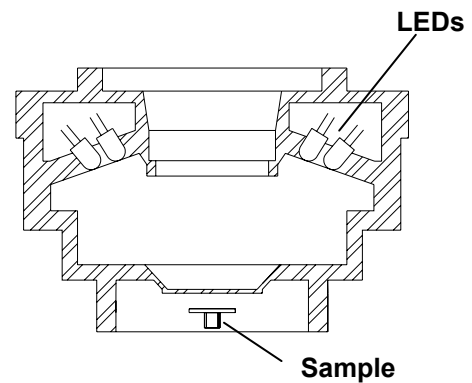


**Figure 11:** Layout of the stimulation unit.

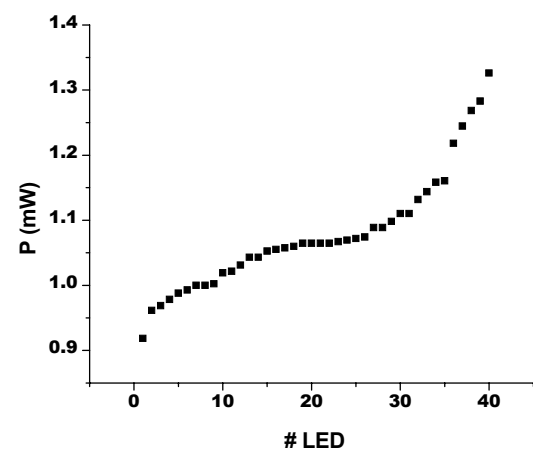


**Figure 12:** Power output of the 40 LEDs employed in the stimulation unit.

To characterize the stimulation unit, it was mounted in the experimental setup (Figure 3) and the illumination pattern was measured (Figure 13). Prior to the measurement, the linearity of the photodiode response had been verified. Figure 14 shows the same data truncated out of the sample zone, where it is observed that the pattern is almost flat. The calculated standard deviation in the sample zone was as low as 1.7 %, which is several times lower than the planned uniformity.

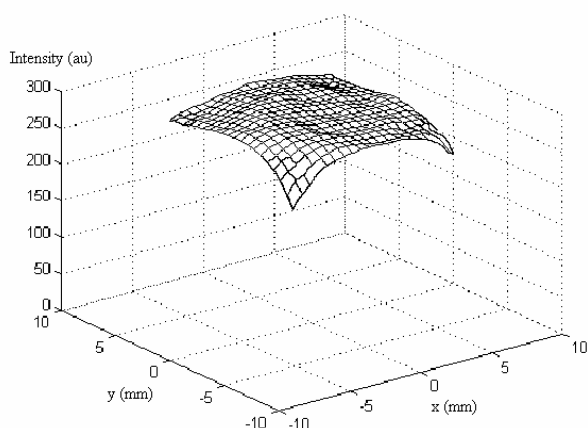


**Figure 13:** Measured illumination pattern in the sample plane.

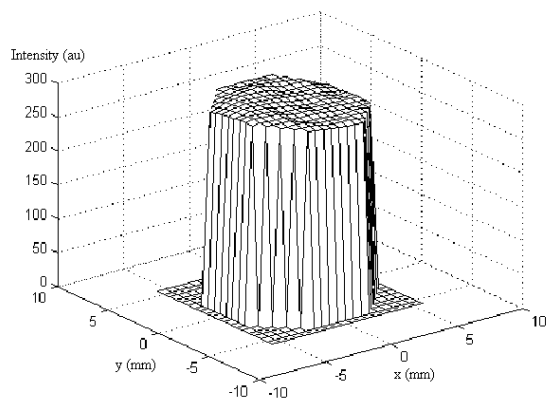


**Figure 14:** Measured illumination pattern in the sample zone.

## Conclusions

A blue LED stimulation unit with a highly uniform illumination pattern was designed and constructed, following the development of a computational tool to allow minimization of the experimental work.

## References

- Bøtter-Jensen L. (2000) *Development of optically stimulated luminescence techniques using natural minerals and ceramics, and their application to Retrospective Dosimetry*. Risø National Laboratory Risø-R-1211(EN), 185 pp.
- Bøtter-Jensen L., Murray A. S. (1999) Developments in optically stimulated luminescence techniques for dating and retrospective dosimetry. *Radiation Protection Dosimetry* **84**, 307-316.
- Bøtter-Jensen L., Duller G. A. T., Murray A. S., Banerjee D. (1999) Blue light emitting diodes for optical stimulation of quartz in retrospective dosimetry and dating. *Radiation Protection Dosimetry* **84**, 335-340.
- Duller G.A.T., Bøtter-Jensen L., Murray A.S. (2000) Optical dating of single sand-sized grains of quartz: sources of variability. *Radiation Measurements* **32**, 453-457.
- Jacobs Z., Duller G. A. T., Wintle A. G. (2003) Optical dating of dune sand from Blombos Cave, South Africa: II –single grain data. *Journal of Human Evolution* **44**, 613-625.

## Reviewer

Ann Wintle